Cobalt-Platinum Heterometallic Clusters Containing N-Heterocyclic Carbene Ligands

Bo Yang Chor,[1,2] Wei Xiang Koh,[1] Rakesh Ganguly,[1] Yongxin Li,[1] Luwei Chen,[2] Robert Raja,[3] and Weng Kee Leong[1,*]

[1]*Division of Chemistry & Biological Chemistry, Nanyang Technological University, 21 Nanyang Link, Singapore 637371.*

[2]*Institute of Chemical and Engineering Sciences, 1 Pesek Road, Singapore 627833*

[3]*School of Chemistry, University of Southampton, Southampton SO17 1BJ, U.K.*

Abstract

The heteronuclear cobalt-platinum cluster $[Co_2Pt_2(IPr)_2(\mu_2\text{-}CO)_4(CO)_4]$ can be obtained through an addition reaction in $[Co_2(CO)_8]$, and with subsequent cluster fragmentation in $[Co_4(CO)_{12}]$ and $[Co_3(\mu_3\text{-}CH)(CO)_9]$, upon reaction with the [Pt(IPr)] fragment. The last reaction also afforded another cobalt-platinum cluster $[Co_4Pt_2(\mu_6\text{-}C)(IPr)_2(\mu_2\text{-}CO)_5(CO)_6]$. These are the first examples of Co-Pt heteronuclear clusters containing NHC ligands.

Keywords: Cobalt; platinum; heteronuclear carbonyl clusters; NHC

Dedicated to Professor Richard D. Adams on his 70th birthday.

1. Introduction

The cobalt-platinum bimetallic system has been known to be effective catalysts for Fischer-Tropsch synthesis [1]. It has also been used as oxidation catalysts, such as, for methanol electro-oxidation in the Direct Methanol Fuel Cell (DMFC), toluene combustion, and preferential CO oxidation reactions [2]. The use of heterometallic carbonyl clusters as a single-source precursor for such bimetallic systems have proven to afford catalysts which show superior performance to those prepared with traditional salt-impregnation methods [3] but to-date, cluster-derived cobalt-platinum catalysts have only been tested for the hydrogenolysis and demethylation of methylcyclopentane [4]. This strategy is, however, contingent upon the availability of suitable cluster precursors thus making the synthesis of heterometallic clusters a desirable endeavour.

* Corresponding author. Tel: +65 6592 7577. E-mail: chmlwk@ntu.edu.sg

Cobalt carbonyl clusters which make suitable precursors for the synthesis of heterometallic clusters with varying metal ratios include $[Co_2(CO)_8]$ (**1**), $[Co_3(\mu_3\text{-}CH)(CO)_9]$ (**2**) and $[Co_4(CO)_{12}]$ (**3**) because they are readily accessible. The addition of unsaturated $[Pt(PR_3)]$ fragments, generated *in situ* via the loss of the ethylene ligand from $[Pt(C_2H_4)_2(PR_3)]$, to cobalt carbonyl clusters have been reported. For example, the reaction with **2** gave two addition products, $[Co_3Pt_2(\mu_2\text{-}H)(\mu_5\text{-}C)(PPr^i_3)_2(CO)_9]$ and $[Co_3Pt_3(\mu_2\text{-}H)(\mu_6\text{-}C)(PPr^i_3)_3(CO)_9]$ (Scheme 1) [5]. In contrast to the chemistry of $[Pt(PR_3)]$ fragments, the addition of [Pt(NHC)] (where NHC = N-heterocyclic carbene) fragments onto cobalt carbonyl clusters is as yet unknown. We recently showed that the reactive [M(NHC)] (where M = Pd or Pt) fragments, generated *in situ* from [M(NHC)(allyl)Cl], could successfully add across Os-Os bonds [6]. Our work with the cobalt carbonyl clusters **1-3** is reported here.

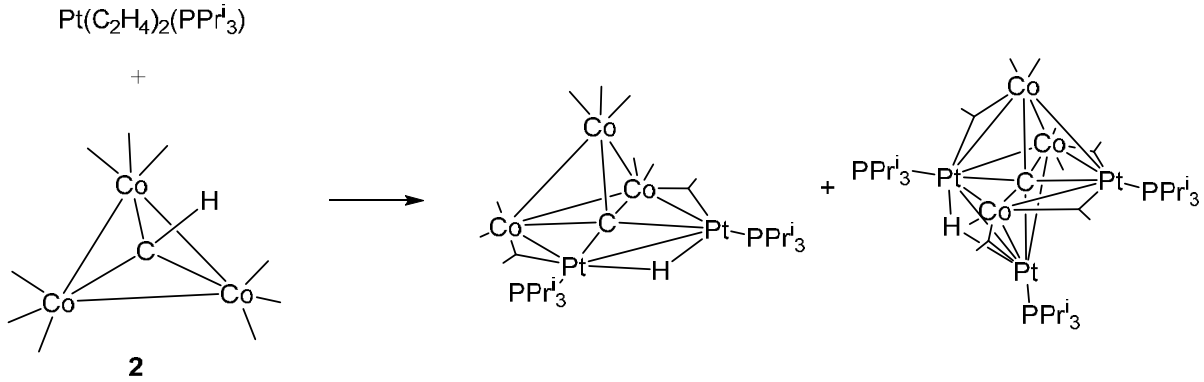

Scheme 1

2. Results and discussion

Room temperature reactions of the [Pt(IPr)] fragment (where IPr = [1,3-bis(2,6-diisopropylphenyl)imidazol-2-ylidene]) (**6**), generated *in situ* from [Pt(NHC)(2-methylpropenyl)Cl], with the cobalt carbonyl clusters **1-3** are summarised in Scheme 2. Both **1** and **3** reacted cleanly with two moles of **6** to afford the cluster $[Co_2Pt_2(IPr)_2(\mu_2\text{-}CO)_4(CO)_4]$ (**4**) as an air-stable, purple solid. The formation of **4** from **1** corresponds to the addition of two units of **6** while in the reaction of **3**, no Co_4Pt_x cluster was observed even with one molar equivalent of **6**. The reaction involving **2** was more complicated, giving multiple products from which only **4** and another new cluster $[Co_4Pt_2(\mu_6\text{-}C)(IPr)_2(\mu_2\text{-}CO)_5(CO)_6]$ (**5**) was isolated as an air-stable, green solid. Interestingly, the IPr analogues of

the phosphine derivatives $[Co_3Pt_2(\mu_2\text{-}H)(\mu_5\text{-}C)(PPr^i_3)_2(CO)_9]$ and $[Co_3Pt_3(\mu_2\text{-}H)(\mu_6\text{-}C)(PPr^i_3)_3(CO)_9]$given in Scheme 1 were not observed, even with various molar equivalents of [Pt(IPr)].

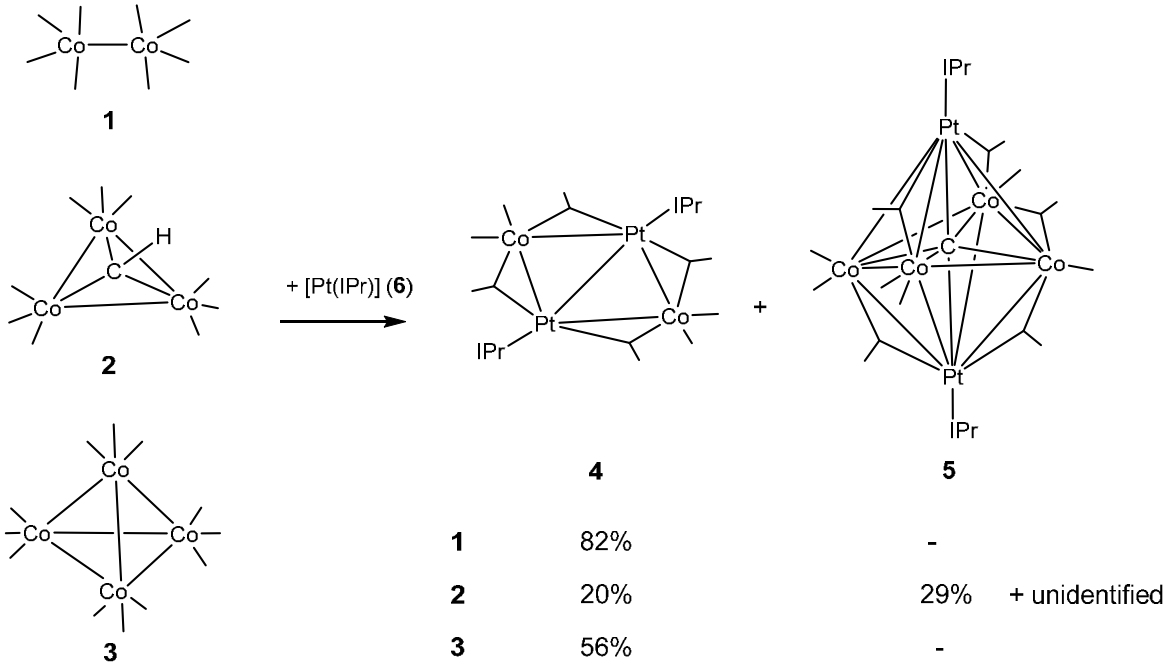

1	82%	-	
2	20%	29%	+ unidentified
3	56%	-	

Scheme 2

The molecular structures of **4** and **5** have been confirmed by single crystal X-ray crystallographic analyses. The ORTEP plot showing the molecular structure of **4**, together with selected bond parameters, is given in Figure 1. The crystal of **4** exhibited disorder about a crystallographic mirror plane passing through the two Pt atoms. The molecule itself is located at a special position with 2/m symmetry, with the 2-fold rotation axis through the Pt atoms. The IR spectrum confirmed the presence of both terminal and bridging CO ligands, while the NMR spectrum showed one set of resonances for the IPr carbene ligand.

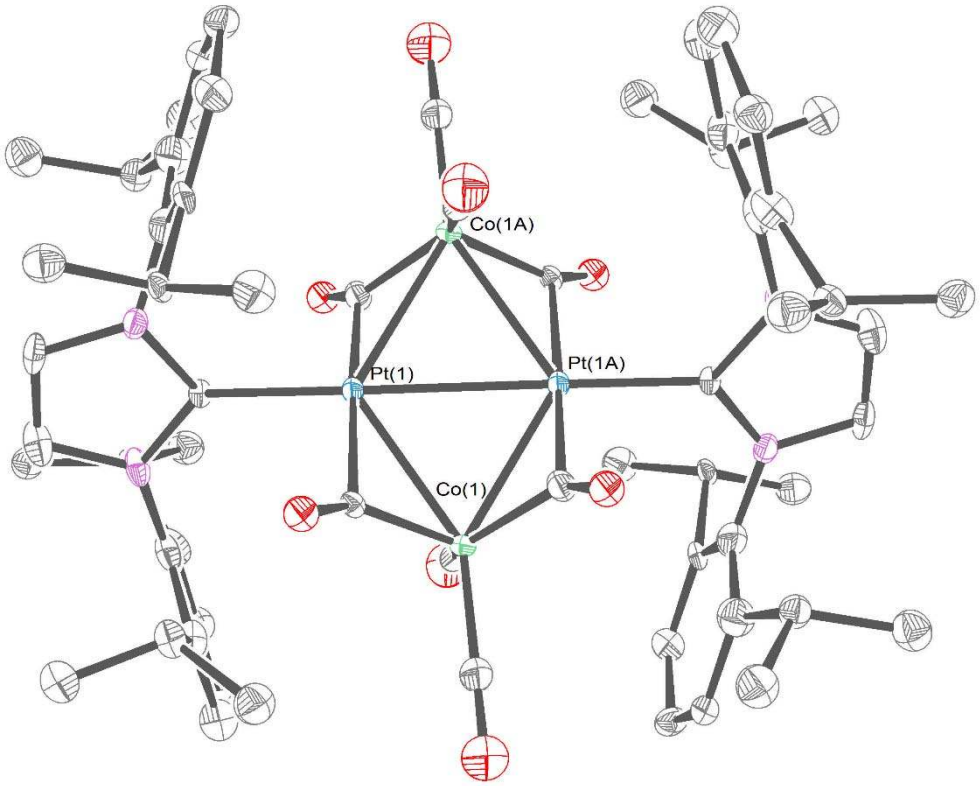

Figure 1. ORTEP diagram of cluster **4**. Ellipsoids are drawn at 50% probability level. Hydrogen atoms have been omitted for clarity. Selected bond lengths (Å) and angles (°): Pt(1)-Pt(1A) = 2.7570(6), Pt(1)-Co(1) = 2.526(2) / 2.58226(2)*, Pt(1)-Co(1A) = 2.5918(19) / 2.5672(19)*, Co(1A)-Pt(1)-Co(1) = 114.83(5) / 115.26(5)*, Co(1)-Pt(1)-Pt(1A) = 58.56(4) / 57.89(4)*, Co(1)-Pt(1)-Pt(1A) = 56.27(5) / 57.37(4)*. *values for the other half of the disorder.

The valence electron count of 58 is in accord with the EAN rule for a 16-electron configuration for Pt. There is a Pt-Pt bonding interaction (Pt(1)-Pt(1A) = 2.7570(6) Å), but no Co-Co bond (Co(1)…Co(1A) ~ 4.349 Å). This contrasts with its phosphine analogue $[Co_2Pt_2(PPh_3)_2(\mu_2\text{-}CO)_3(CO)_5]$ (**4'**) which has a butterfly Co_2Pt_2 core, an intact Co-Co bond (2.498(3) Å) and a Pt…Pt distance of 2.987(4) Å [7] (Figure 2). In comparison, the Co_2Pt_2 core in **4** is constrained by the crystallographic 2/m symmetry to be planar. This difference in skeletal arrangement is not uncommon in heteronuclear clusters, however. For example, while $[Mo_2Pt_2(\eta_5\text{-}C_5H_5)_2(PEt_3)_2(\mu_2\text{-}CO)_6]$ has a planar Mo_2Pt_2 core, the PPh_3 analogue $[Mo_2Pt_2(\eta_5\text{-}C_5H_5)_2(PPh_3)_2(\mu_2\text{-}CO)_4(CO)_2]$ has a butterfly core [8]. Interconversion in

solution between skeletal isomers is also possible, for example, the bulkier phosphine analogues $[Mo_2Pt_2(\eta_5\text{-}C_5H_4Me)_2(PR_3)_2(CO)_6]$ (R = Cy or Pr^i) can exist in solution with both a planar and a tetrahedral core [9], although there is no evidence of this for cluster **4**.

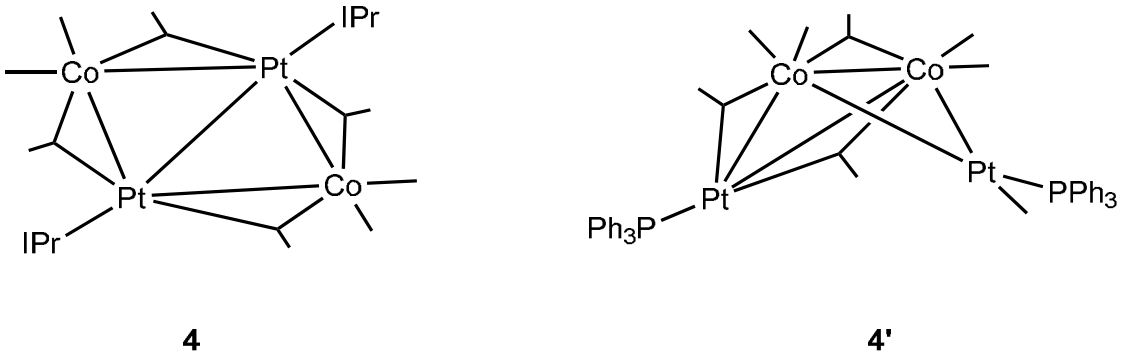

4 **4'**

Figure 2. Molecular structures of **4** and **4'**.

The ORTEP plot showing the molecular structure of **5**, together with selected bond parameters, is given in Figure 3. IR analysis confirmed the presence of both terminal and bridging CO ligands, while the NMR spectrum showed one set of resonances for the IPr carbene, consistent with the symmetry of the cluster. The $Co_4Pt_2(\mu_6\text{-}C)$ core is a distorted octahedron, in accord with PSEPT for a cluster valence electron count of 86, and the puckered basal plane is made up of the four cobalt atoms. This molecular geometry closely resembles that of the only known [Pd(PPh$_3$)] analogue, $[Co_4Pd_2(\mu_6\text{-}C)(PPh_3)_2(\mu_2\text{-}CO)_5(CO)_6]$ (**5'**) [10] (Figure 4).

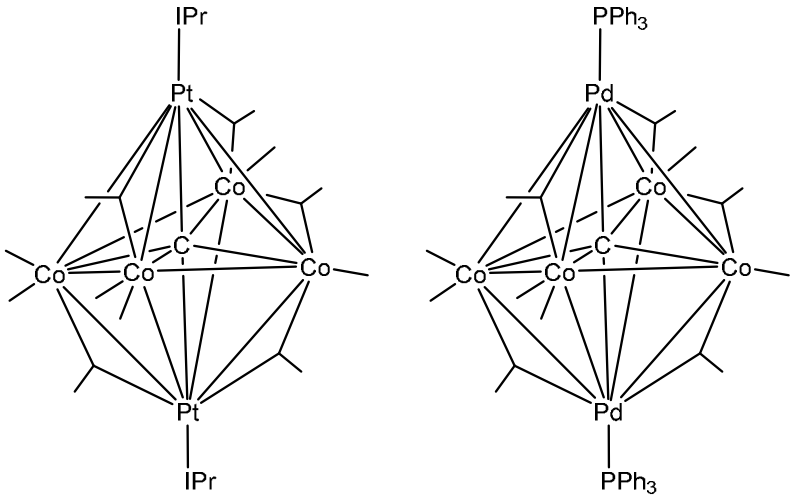

5 **5'**

Figure 4. Molecular structure of cluster **5** and **5'**.

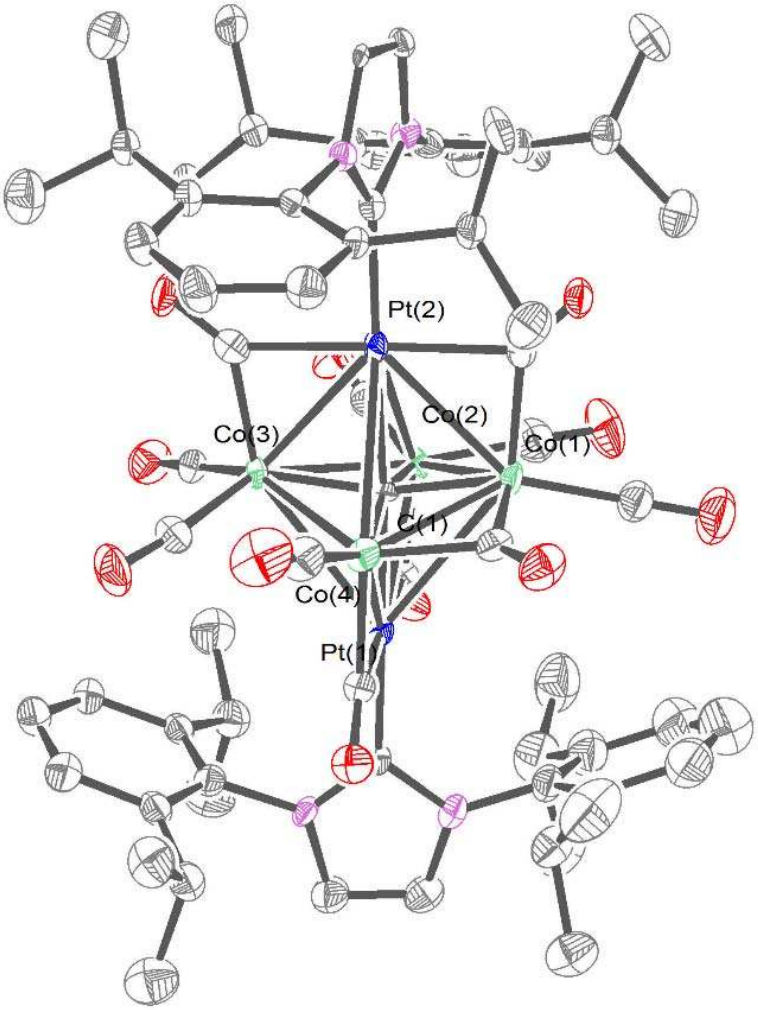

Figure 3. ORTEP diagram of cluster **5**. Ellipsoids are drawn at 50 % probability level. Hydrogen atoms have been omitted for clarity. Selected bond lengths (Å): Co(1)-C(1) = 1.880(13), Co(2)-C(1) = 1.846(12), Co(3)-C(1) = 1.846(13), Co(4)-C(1) = 1.869(12), Pt(1)-C(1) = 2.123(12), Pt(2)-C(1) = 2.142(12), Co(1)-Co(2) = 2.705(3), Co(1)-Co(4) = 2.518(3), Co(2)-Co(3) = 2.698(2), Co(3)-Co(4) = 2.692(3), Co(1)-Pt(2) = 2.6359(19), Co(2)-Pt(2) = 2.9791(18), Co(3)-Pt(2) = 2.6322(19), Co(4)-Pt(2) = 3.0428(19), Co(2)-Pt(1) = 2.6389(19), Co(3)-Pt(1) = 2.8972(18), Co(4)-Pt(1) = 2.6401(19) , Co(1)-Pt(1) = 3.1303.

The Co-$C_{carbide}$ and Co-Co bond lengths (1.846(12) - 1.869(12) and 2.518(3) - 2.705(3) Å, respectively) in **5** are comparable to those in the homometallic, octahedral cluster $[Co_6(\mu_6\text{-}C)(CO)_{13}]^{2-}$ (1.852(3) - 1.880 and 2.4618(8) - 2.926(1) Å, respectively) [11]. The Pt-$C_{carbide}$ and the Co-Pt bond lengths (2.123(12) - 2.142(12) and 2.6322(19)Å - 3.1303(2) Å, respectively) in **5** are also comparable to those found in $[Co_3Pt_3(\mu\text{-}H)(\mu_6\text{-}C)(PPr^i_3)_3(CO)_9]$ (2.04(1) - 2.16(1) and 2.598(3) - 3.060(3) Å, respectively) [5]. One of the Co-Pt bonds (Pt(1)-Co(1) = 3.1303(2) Å) is unusually long, which we believe may be due to the effects of crystal packing forces. An attempt was made to corroborate this via a natural bond orbital (NBO) analysis on **5** with density functional theory (DFT) at the def2SVP/6-31G* level of theory. The Wiberg bond indices and metal-metal bond lengths for the optimised geometry are given in Figure 5.

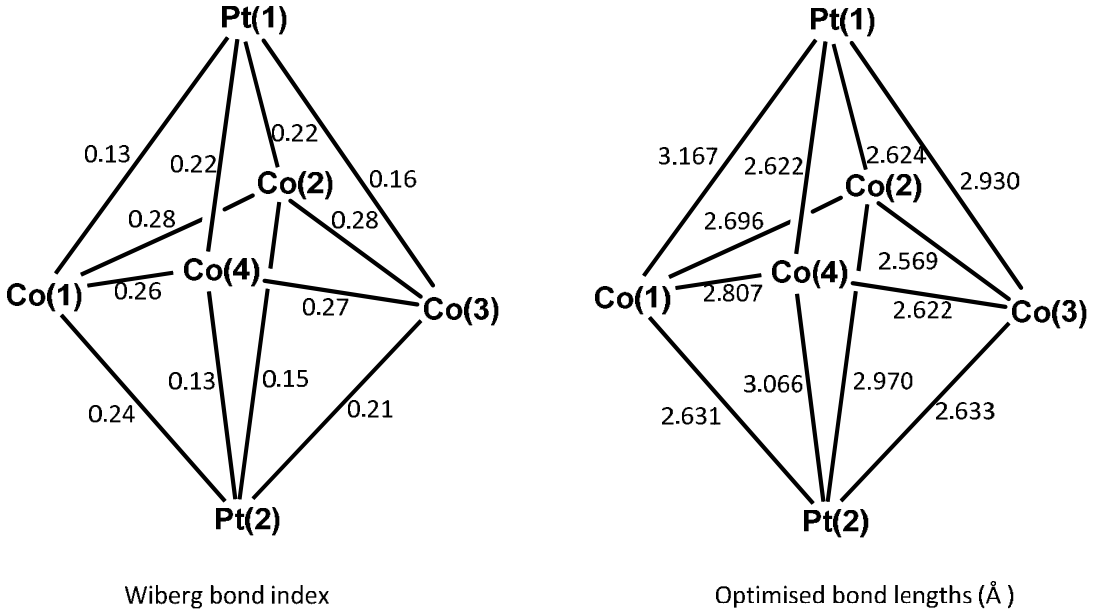

Figure 5. Wiberg bond indices (left) and calculated metal-metal bond lengths in Å (right) for cluster **5**.

The bond indices for the Co-Pt bonds can be divided into two sets, with values in the ranges 0.13-0.16 (Pt(1)-Co(1), Pt(1)-Co(3), Pt(2)-Co(4) and Pt(2)-Co(2)), and 0.21-0.24 (Pt(1)-Co(4), Pt(1)-Co(2), Pt(2)-Co(1) and Pt(2)-Co(2)). They correlate well with both the calculated and experimental bond lengths; those with shorter bond lengths correspond to higher bond indices, in accord with the trend reported for metal-metal bonds [12]. Although there are no reports of bond indices for Co-Pt bonds, it has been reported that homonuclear metal-metal bonds such as the single Ru-Ru bond has

bond index ~0.2 [13], and that for a single Fe-Fe bond has bond index ~0.1 [14]. The bond indices calculated here thus suggest that the Pt(1)-Co(1) vector corresponds to a single metal-metal bond.

The formation of **4** and **5** requires a change in the nuclearity of the reactants **1-3**. This may be attributed to the ease with which cobalt carbonyl clusters undergo cluster fragmentation/rearrangement and is not unprecedented. For example, reaction of the cluster $[Co_6(\mu_6\text{-}C)CO)_{15}]^{2-}$ with a lower molar equivalent of $[Au(PPh_3)Cl]$ afforded a Co_6Au_x cluster, while use of a larger molar equivalent resulted in a reduction in nuclearity to afford Co_4Au_x and Co_5Au_x clusters [15]. In analogy to $[Co_4Au_2(\mu_6\text{-}C)(PPh_3)_2(CO)_{10}]$, which has been regarded as a stabilized form of the unobserved anionic cluster $[Co_4(\mu_4\text{-}C)(CO)_{10}]^{2-}$ by two $[Au(PPh_3)]^+$ fragments [15], the formation of **5** from **2** may thus be viewed as the stabilisation of the unobserved, neutral cluster $[Co_4(\mu_4\text{-}C)(CO)_{11}]$ by two [Pt(IPr)] fragments.

3. Concluding remarks

In this work, we reported that a [Pt(NHC)] fragment could react with a variety of cobalt carbonyl clusters (**1-3**) to give new heteronuclear cobalt-platinum clusters. The results show that the [Pt(NHC)] fragment added across Co-Co bonds but as is characteristic of cobalt carbonyl clusters, the reactions were accompanied by cluster fragmentation/rearrangement, and appeared to favour the formation of clusters **4** and **5** which presumably corresponded to "thermodynamic sinks" for these reactions.

4. Experimental

4.1. General procedure

All reactions were performed under an argon atmosphere using standard Schlenk techniques or in a glove box. Solvents used in reactions were of AR grade, and were dried over the appropriate drying agent, distilled under nitrogen and stored in flasks fitted with Teflon valves prior to use. Preparative TLC separations were carried out on Merck silica gel 60 Å F 254 20 × 20 cm^2 plates. ^1H NMR spectra were collected on a Bruker BBFO 400 or AV 300 NMR spectrometer, with chemical shifts referenced to the solvent residual peaks. High resolution mass spectra were recorded in electrospray ionization

(ESI) mode on a Waters UPLC-Q-TOF mass spectrometer. Elemental analyses were performed by the microanalytical laboratory in NTU. $[Co_2(CO)_8]$ (**1**) and $[Co_4(CO)_{12}]$ (**1**) were purchased from Alfa Aesar, and the complexes $[Co_3(\mu_3\text{-CH})(CO)_9]$ (**2**) [16] and $[PtIPr(C_4H_7)Cl]$ (**6**) [17] were prepared according to published methods. All other reagents were used as received from commercial suppliers.

4.2. Reaction of 1 with [Pt(IPr)]

A sample of **6** (30.0 mg, 0.0445 mmol) and KO^{t}Bu (5.0 mg, 0.045 mmol) in IPA (5 mL) were heated at 80 ^{o}C for 1 h during which the initial colourless solution turned yellow. After removal of the solvent under vacuum, the yellow oil was re-dissolved in toluene (10 mL) to which **1** (7.6 mg, 0.022 mmol) was added. The solution turned red-purple and was left to stir at RT for 3 h. After removal of the solvent, the residue was re-dissolved in the minimum volume of toluene and filtered through a thin pad of silica gel. The solvent was then removed, and the residue washed with hexane followed by extraction with diethyl ether. Removal of the ether afforded a purple solid which was recrystallized from a DCM/hexane solvent mixture to give $[Co_2Pt_2(IPr)_2(\mu_2\text{-CO})_4(CO)_4]$ (**4**) as purple crystals. (Yield = 27.4 mg, 82%). IR (Et_2O): ν_{CO} 2034 (w), 2018 (s), 2002 (w), 1978 (vs), 1942 (vw), 1837 (m), 1817 (s), 1796 (w) cm^{-1}. ^{1}H NMR (300 MHz, C_6D_6): δ 7.08 (d, 4H, *meta*-Ar-**H**), 6.52 (t, 2H, Imidazole **H**), 2.97 (sept, 4H, C**H**$(CH_3)_2$), 1.44 (dd, 12H, CH(C**H**$_3)_2$), 0.92 (dd, 12H, CH(C**H**$_3)_2$). ESI-MS$^+$ m/z: 1285.39 $[M\text{-}8CO]^+$. Analysis (%): C 48.16, H 4.98, N 3.53 (found); C 48.38, H 4.74, N 3.61 (calcd for $C_{62}H_{72}Co_2N_4O_8Pt_2{\cdot}0.5CH_2Cl_2$).

4.3. Reaction of 2 with [Pt(IPr)]

A solution of **6** (19.5 mg, 0.0289 mmol) and KO^{t}Bu (3.3 mg, 0.029 mmol) in IPA (10 mL) was heated at 80 ^{o}C for 1 h to give a yellow solution. The solvent was removed under vacuum to give a yellow oil which was redissolved in DCM (10 mL) to which **2** (6.2 mg, 0.014 mmol) was added. The reaction mixture was stirred at RT for 15 h during which the solution turned dark brown. After removal of the solvent, the residue was re-dissolved in a minimum volume of DCM and separated by TLC with hexane:DCM (5:2, v/v) as the eluent. Two major bands were isolated and characterized.

The first major band afforded a green solid which was recrystallized from diethyl ether to afford $[Co_4Pt_2(\mu_6\text{-}C)(IPr)_2(\mu_2\text{-}CO)_5(CO)_6]$ (**5**) as dark green crystals. (Yield = 5.4 mg, 29%). IR (DCM): ν_{CO} 2047 (vw), 2010 (vs), 1846 (m), 1819 (m, sh) cm^{-1}. ^1H NMR (400 MHz, $CDCl_3$): δ 7.05 (d, 4H, *meta*-Ar-**H**), 6.73 (t, 2H, Imidazole **H**), 2.97 (sept, 4H, C**H**$(CH_3)_2$), 1.43 (dd, 12H, CH(C**H**$_3)_2$), 0.89 (dd, 12H, CH(C**H**$_3)_2$). ESI-MS^+ m/z: 1723.25 $[M]^+$, 1695.26 $[M\text{-}CO]^+$, 1639.25 $[M\text{-}3CO]^+$.

The second purple-brown band yielded a purple solid which was identified to be cluster **4** by its IR spectrum. (Yield = 3.3 mg, 20%).

4.4. Reaction of 3 with [Pt(IPr)]

A sample of **6** (21.1 mg, 0.0329 mmol) and KO^tBu (3.5 mg, 0.033 mol) were heated to 80 ^oC in IPA (5 mL) for 1 h. The yellow oil obtained after removal of the solvent was re-dissolved in toluene (10 mL) to which **3** (5.97 mg, 0.0104 mmol) was added. The reaction mixture was left to stir for 15 h during which it turned to purple-brown. After removal of the solvent, the residue was re-dissolved in a minimum amount of DCM and separated by TLC with hexane:DCM (1:1, v/v) as eluent to afford **4** as the major product. (Yield = 17.8 mg, 56%).

4.5. X-ray crystallographic studies

The crystals were mounted on quartz fibres. X-ray data were collected at 103 K on a Bruker Kappa diffractometer equipped with a CCD detector, employing Mo Kα radiation (λ = 0.71073 Å), with the SMART suite of programs [18]. The data was processed and corrected for Lorentz and polarisation effects with SAINT [19], and for absorption effects with SADABS [20]. Structural solution and refinement were carried out with the SHELXTL suite of programs [21]. The structures were solved by direct or Patterson methods to locate the heavy atoms, followed by successive difference maps for the light, non-hydrogen atoms. All non-hydrogen atoms were refined with anisotropic thermal parameters in the final model.

The crystal of **4** exhibited disorder of the diisopropylphenyl groups as well as the CO ligands and the cobalt atoms. These were modeled with two alternative sites each, with equal occupancies, and

appropriate restraints were applied. A diethyl ether solvate was found in the asymmetric unit of the crystal of **5**. Crystal and refinement data are summarized in Table 1.

4.6. Computational studies

Computational studies were carried out with the Gaussian 09W suite of programs, with the M06L density functional, utilizing def2SVP basis set for Pt atoms, while the 6-31G* basis set is used for the remaining atoms [22]. Natural Bond Orbital (NBO) analysis was carried out with the NBO 3.1 program implemented within Gaussian 09W [23].

Acknowledgements

This work was supported by Nanyang Technological University and the Ministry of Education (Research Grant No. M4011158). BYC thanks the Agency for Science, Technology and Research (A*STAR, Singapore) for a Graduate Scholarship.

Supplementary material: Crystallographic data (excluding structure factors) for the structures in this paper have been deposited with the Cambridge Crystallographic Data Centre as supplementary publication numbers CCDC 1532322 and 1532323 for **4** and **5**, respectively. Copies of the data can be obtained, free of charge, on application to CCDC, 12 Union Road, Cambridge CB2 1EZ, UK, (fax: +44 1223 336033 or e-mail: deposit@ccdc.cam.ac.uk).

Table S1. Crystal and structure refinement data for complexes **4** and **5**.

Complex	**4**	**5**
Empirical formula	$C_{62}H_{72}Co_2N_4O_8P_{t2}$	$C_{66}H_{72}Co_4N_4O_{12}Pt_2.Et_2O$
Formula weight	1509.28	1797.29
Crystal system	Monoclinic	Monoclinic
Space group	P 2_1/n	P 2_1/n
a, Å	13.048(2)	12.5072(15)
b, Å	14.253(2)	31.460(4)
c, Å	16.460(3)	18.748(3)
β, deg	98.476(12)	102.637(5)
Volume, $Å^3$	3027.8(8)	7198.3(15)
Z	2	4
Density (calculated), Mg/m^3	1.655	1.658
Absorption coefficient, mm^{-1}	5.200	4.832
F(000)	1492	3560
Crystal size, mm^3	0.22 x 0.12 x.0.10	0.34 x 0.14 x 0.06
Reflections collected	47666	119217
Independent reflections	6186 [R(int) = 0.1315]	14704 [R(int) = 0.1698]
Max. and min. transmission	0.6244 and 0.3942	0.76 and 0.29
Data / restraints / parameters	6186 / 566 / 473	14704 / 516 / 847
Goodness-of-fit on F^2	1.094	1.197
Final R indices [I>2s(I)]	R1 = 00417 wR2 = 0.0.0986	R1 = 0.0792 wR2 = 0.1679
R indices (all data)	R1 = 0.0676 wR2 = 0.1257	R1 = 0.1264 wR2 = 0.1893
Largest diff. peak and hole, $e.Å^{-3}$	1.362 and -1.534	2.772 and -3.165

Reference

1 (a) J.H. den Otter, H. Yoshida, C. Ledesma, D. Chen, K.P. de Jong, J. Catal. 340 (2016) 270-275. (b) J.H. den Otter, S.R. Nijveld, K.P. de Jong, ACS Catalysis 6 (2016) 1616-1623. (c) V. Montes, M. Boutonnet, S. Järås, M. Lualdi, A. Marinas, J.M. Marinas, F.J. Urbano, M. Mora, Catal. Today 223 (2014) 66-75.

2 (a) A. Nouralishahi, A.M. Rashidi, Y. Mortazavi, A.A. Khodadadi, M. Choolaei, Appl. Surf. Sci. 335 (2015) 55-64. (b) V. Kepenienė, L. Tamašauskaitė-Tamašiūnaitė, J. Jablonskienė, M. Semaško, J. Vaičiūnienė, R. Vaitkus, E. Norkus, Mater. Chem. Phys. 171 (2016) 145-152. (c) H. Yang, J. Deng, Y. Liu, S. Xie, P. Xu, H. Dai, Chinese Journal of Catalysis 37 (2016) 934-946. (d) X. Yu, H. Li, S.-T. Tu, J. Yan, Z. Wang, Int. J. Hydrogen Energy 36 (2011) 3778-3788. (e) A. López, N. Navascues, R. Mallada, S. Irusta, Appl. Catal., A 528 (2016) 86-92.

3 See, for example: (a) B. F. G. Johnson, Coord. Chem. Rev. 190–192 (1999) 1269. (b) B.F.G. Johnson, Top. Catal. 24 (2003) 147. (c) J. M. Thomas, B.F.G. Johnson, R. Raja, G. Sankar, P.A. Midgley, Acc. Chem. Res. 36 (2003) 20. (d) A. C. W. Koh, W.K. Leong, L. Chen, T.P. Ang, J. Lin, B.F.G. Johnson, T. Khimyak, Catal. Commun. 9 (2008) 170. (e) S. Zacchini, Eur. J. Inorg. Chem. (2011) 4125. (f) P. Buchwalter, J. Rosé, P. Braunstein, Chem. Rev. 115 (2015) 28.

4 P. Buchwalter, J. Rosé, P. Braunstein, Chem. Rev. 115 (2015) 28-126.

5 J.C. Jeffery, M.J. Parrott, F.G.A. Stone, J. Organomet. Chem. 382 (1990) 225-235.

6 (a) Y. Liu, R. Ganguly, H.V. Huynh, W.K. Leong, Organometallics 32 (2013) 7559-7563. (b) Y. Liu, PhD thesis, Nanyang Technological University, (2014).

7 J. Fischer, A. Mitschler, R. Weiss, J. Dehand, J.F. Nennig, J. Organomet. Chem. 91 (1975) C37-C38.

8 (a) R. Bender, P. Braunstein, Y. Dusausoy, J. Protas, J. Organomet. Chem. 172 (1979) C51-C54. (b) F.G.A. Stone, Inorg. Chim. Acta 50 (1981) 33-42.

9 P. Braunstein, C. De Meric de Bellefon, S.E. Bouaoud, D. Grandjean, J.F. Halet, J.Y. Saillard, J. Am. Chem. Soc. 113 (1991) 5282-5292.

10 I. Ciabatti, F. Fabrizi de Biani, C. Femoni, M.C. Iapalucci, G. Longoni, S. Zacchini, ChemPlusChem 78 (2013) 1456-1465.

11 V.G. Albano, D. Braga, S. Martinengo, J. Chem. Soc., Dalton Trans. (1986) 981-984.

12 V. Singh, M. Dixit, M. Kosa, D.T. Major, E. Levi, D. Aurbach, Chem. Eur. J. 22 (2016) 5269-5276.

13 (a) E.P. Fowe, B. Therrien, G. Süss-Fink, C. Daul, Inorg. Chem. 47 (2008) 42-48. (b) S.P. Oh, B.Y. Chor, W.Y. Fan, Y. Li, W.K. Leong, Organometallics 30 (2011) 6774-6777.

14 H. Wang, Y. Xie, R.B. King, H.F. Schaefer, J. Am. Chem. Soc. 128 (2006) 11376-11384.

15 I. Ciabatti, C. Femoni, M. Hayatifar, M.C. Iapalucci, S. Zacchini, Inorg. Chim. Acta 428 (2015) 203-211.

16 (a) T. Sugihara, A. Wakabayashi, Y. Nagai, H. Takao, H. Imagawa, M. Nishizawa, Chem. Commun. (2002) 576-577. (b) M.O. Nestle, J.E. Hallgren, D. Seyferth, P. Dawson, B.H. Robinson, Inorg. Synth. 20 (1980) 226-229.

17 S. Fantasia, S.P. Nolan, Chem. Eur. J. 14 (2008) 6987-6993.

18 *SMART Version 5.628*, Bruker AXS Inc., Madison, Wisconsin, USA, 2001.

19 *SAINT+ Version 6.22a*, Bruker AXS Inc, Madison, Wisconsin, USA, 2001.

20 Sheldrick, G.M. SADABS; University of Göttingen, Göttingen, Germany, 1996.

21 SHELXTL Version 5.1, Bruker AXS Inc, Madison, Wisconsin, USA, 1997.

22 M.J. Frisch, G.W. Trucks, H.B. Schlegel, G.E. Scuseria, M.A. Robb, J.R. Cheeseman, G. Scalmani, V. Barone, B. Mennucci, G.A. Petersson, H. Nakatsuji, M. Caricato, X. Li, H.P. Hratchian, A.F. Izmaylov, J. Bloino, G. Zheng, J.L. Sonnenberg, M. Hada, M. Ehara, K. Toyota, R. Fukuda, J. Hasegawa, M. Ishida, T. Nakajima, Y. Honda, O. Kitao, H. Nakai, T. Vreven, J.A. Montgomery, P.J.J. E., F. Ogliaro, M. Bearpark, J.J. Heyd, E. Brothers, K.N. Kudin, V.N. Staroverov, R. Kobayashi, J. Normand, K. Raghavachari, A. Rendell, J.C. Burant, S.S. Iyengar, J. Tomasi, M. Cossi, N. Rega, J.M. Millam, M. Klene, J.E. Knox, J.B. Cross, V. Bakken, C. Adamo, J. Jaramillo, R. Gomperts, R.E. Stratmann, O. Yazyev, A.J. Austin, R. Cammi, C. Pomelli, J.W. Ochterski, R.L. Martin, K. Morokuma, V.G. Zakrzewski, G.A. Voth, P. Salvador, J.J. Dannenberg, S. Dapprich, A.D. Daniels, Ö. Farkas, J.B. Foresman, J.V. Ortiz, J. Cioslowski, D.J. Fox, Gaussian 09, revision D.01, Gaussian, Inc., Wallingford CT (2009).

23 E.D. Glendening, A.E. Reed, J.E. Carpenter, F. Weinhold, The NBO 3.1 program.